Journal of the American College of Cardiology
© 1999 by the American College of Cardiology
Published by Elsevier Science Inc.

Vol. 35, No. 1, 1999
ISSN 0735-1097/99/$20.00
PII S0735-1097(99)00498-2

# Stereolithographic Biomodeling to Create Tangible Hard Copies of Cardiac Structures from Echocardiographic Data

## In Vitro and In Vivo Validation

Thomas M. Binder, MD,* Deddo Moertl, MD,* Gerald Mundigler, MD,* Gerhard Rehak,* Manfred Franke,* Georg Delle-Karth, MD,* Werner Mohl, MD,† Helmut Baumgartner, MD, FACC,* Gerald Maurer, MD, FACC*

*Vienna, Austria*

**OBJECTIVES** This study investigated the feasibility, accuracy and clinical potential of creating polymer hard copies of echocardiographic data using stereolithography.

**BACKGROUND** Three-dimensional (3D) echocardiography has so far been limited by the need to display reconstructed 3D objects on a two-dimensional screen. Thus, tangible stereolithographic polymer models created from echocardiographic data could enhance our spatial perception of cardiac anatomy and pathology.

**METHODS** Hard-copy replicas of water-filled latex balloon phantoms (n = 7) and porcine liver specimens (n = 12) were generated from echocardiographic images using stereolithography (computerized laser polymerization). In addition, we created 24 models of the mitral valve from 12 transesophageal studies (normal = 6, mitral stenosis n = 4, prolapse/flail leaflet n = 8, annular dilation n = 2, leaflet restriction n = 2 and following mitral valve repair n = 2).

**RESULTS** Excellent agreement was found for comparison of volumes (r = 0.98, SEE = 3.46 $mm^3$, mean difference = 0.25 ± 3.33 $mm^3$) and maximal dimensions (r = 0.99, SEE = 0.16 cm, mean difference = 0.03 ± 0.16 cm) between phantoms and their corresponding replicas. Visual and tactile examination of mitral valve models by two blinded observers allowed correct depiction of mitral valve anatomy and pathology in all cases.

**CONCLUSIONS** Stereolithographic modeling of echocardiographic images is feasible and provides tangible polyacrylic models that are true to scale, shape and volume. Such models offer accurate depiction of mitral valve anatomy and pathology in patients studied with transesophageal echocardiography. This technique could have substantial impact on diagnosis, management and preoperative planning in complex cardiovascular disorders. (J Am Coll Cardiol 1999;35: 230–7) © 1999 by the American College of Cardiology

Despite numerous reports on the clinical potential of three-dimensional (3D) echocardiography, this method has found only limited application in routine clinical practice (1–5). This may in part be related to present limitation of 3D echocardiography, such as the considerable expertise and time necessary to define representative image planes for reconstruction, difficulties in the interpretation of 3D images that are not truly 3D but virtual two-dimensional (2D) images on a flat computer screen, and finally the complexity of reconstruction algorithms that greatly influence the way structures are perceived (6). Thus, even holographic methods have been applied (7,8) to convey information about the 3D structure of objects.

Ultimately, true 3D representation of cardiac structures may better be achieved by creating tangible models. Such models can serve as a hard copy of echocardiographic data sets and could provide both visual and tactile information of cardiac structures that may enhance the currently employed display on a computer screen.

Stereolithography, a computerized, laser-induced polymerization process, creates polyacrylic models from computer-aided design (CAD) drawings. Such models are now increasingly used by industry to design components for numerous applications, including automobiles, aircrafts and computers. Recently, this technique has also been applied in medicine, mostly to create replicas of skeletal structures from computer tomography (CT) scans (9,10) to aid in complex maxillofacial surgery and orthopedic surgical pro-

From the *Department of Cardiology and †Department of Cardiovascular Surgery, University of Vienna, AKH, Vienna, Austria. No financial support was received for this study.

Manuscript received March 17, 1999; revised manuscript received July 27, 1999, accepted September 14, 1999.

**Abbreviations and Acronyms**

2D = two-dimensional
3D = three-dimensional
CAD = computer-aided design
CT = computer tomography
ECG = electrocardiogram
MV = mitral valve
NIH = National Institutes of Health
SEE = standard error of the estimate
TEE = transesophageal echocardiography

cedures to create "accurate to fit" osteosynthetic grafts (11–13).

Despite its increasing use in various medical fields, the application of stereolithography in cardiology so far has been very limited. This study was performed to test the hypothesis that transesophageal echocardiographic data can be used to create precise 3D models of cardiac structures such as mitral valves (MVs). Thus, we developed a prototype interface between echocardiography and stereolithography to create tangible polyacrylic models in both in vitro and in vivo settings. We sought to validate measurements obtained from the models and to determine whether diagnostic information can be provided for cardiac structures such as MVs.

## METHODS

**In vitro validation.** Seven latex balloons were filled with saline solution to create phantoms with varying sizes (ranging from 9.0 to 75 $cm^3$). The balloons were suspended into a water tank and scanned with a HP Sonos 5500 ultrasound system (Hewlett-Packard, Andover, Massachusetts) using a multiplane TEE probe (5.0 to 6.2 MHz) interfaced to 3D image acquisition software (TomTec, Unterschleissheim, Germany). Ninety planes were recorded during a 180° rotational scan (2° increments) and stored on a magneto-optical disc.

Porcine liver tissue was fixated with 4% formaldehyde solution. From these, 12 specimens with varying shapes and sizes (0.9 to 7.2 cm length, 1.4 to 25.8 $cm^3$ volume) were prepared. The specimens were suspended into a water tank and imaged with the described instrumentation. Volumes of the balloons and liver specimens were determined by water-displacement method.

**In vivo studies.** Transesophageal 3D echocardiography was performed in 13 patients (14 studies) with the instrumentation described above to obtain 3D data sets of the MV. Written informed consent was obtained from all individuals. Five studies were performed in the operating room under general anesthesia, three in the intensive care unit and six in an ambulatory setting. Eight patients were mechanically ventilated at the time of the study. All 13 patients were in sinus rhythm; however, one patient developed atrial fibrillation during the acquisition procedure. The clinical indications for the transesophageal echocardiography (TEE) study and the MV abnormalities that were found during the procedure are listed in Table 1.

**Image processing.** The recorded data sets were transferred to a 3D workstation (TomTec, Unterschleissheim, Germany) for postprocessing. For in vivo studies, end-systolic and end-diastolic frames were selected. The region of interest was defined and extracted from the data set. The image review feature of the system was applied to define the long axis of the structure (phantom, specimen or MV). Perpendicular equidistant short axis cut planes of the data set were reconstructed in predefined intervals along the long axis. These images were then exported to an image analysis environment (NIH [National Institutes of Health] Image

**Table 1.** Study Population

| Patient | Gender | Age | Indication | Morphology | Setting |
|---|---|---|---|---|---|
| PF | m | 56 | Source of embolism | Normal MV | Amb |
| BH | f | 72 | MR | MR restricted leaflet/MS | Amb |
| ST | m | 48 | Dilated cardiomyopathy, MR | Annular dilation | ICU* |
| KG | m | 33 | MR | MVP/flail postleaflet | OP* |
| HK | f | 50 | Endocarditis | Normal MV | ICU* |
| BL | m | 40 | Dissection of Ao | Normal MV | ICU* |
| PK | f | 28 | MR | Flail post-MV leaflet | OP* |
| PK | f | 28 | Post-OP study | Following MV repair | OP* |
| DN | f | 48 | MS | Severe MS | OP* |
| MM | m | 60 | MR | Flail postleaflet | Amb |
| HG | m | 64 | MR | Flail anterior leaflet | OP* |
| PP | m | 48 | MR | Bileaflet MVP | Amb‡ |
| UH | f | 68 | MS | Moderate to severe MS | Amb |
| FZ | m | 72 | AV prosth, endocarditis | Bileaflet MVP | Amb‡ |

*Study was performed under respiratory therapy, ‡3D study not suitable for stereolithographic modeling.
Amb = ambulatory; Ao = aorta; Av prosth = aortic valve prosthesis; ICU = intensive care unit; MR = mitral regurgitation; MS = mitral stenosis; MV = mitral valve; MVP = mitral valve prolapse; OP = intraoperative study.

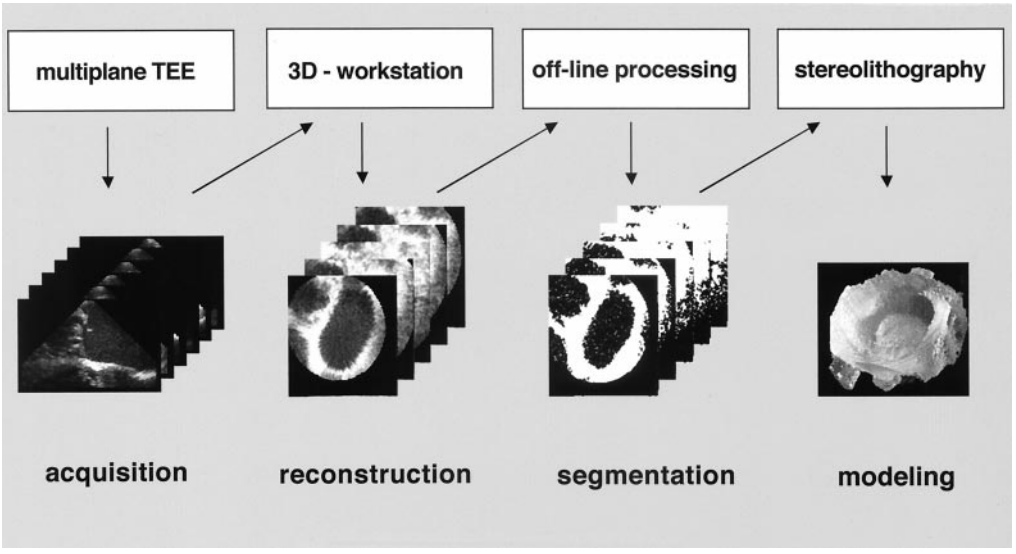


**Figure 1.** Image processing procedure: A rotational TEE scan is performed to acquire a volumetric data set. The images are transferred to a 3D workstation for postprocessing to reconstruct paraplane images. Image segmentation is performed off-line. The segmented images are then exported to the stereolithograph where they serve as a digital 3D pattern to create physical models.

software, version 6.25) where image segmentation using gray scale thresholding was performed to extract actual structures from speckle noise (background). The segmented images were then interfaced to the stereolithograph (Fig. 1). The pixel size and slice thickness (distance between short axis cut planes) were recorded and used by the stereolithograph to compute the dimensions of the model.

**Stereolithography.** Modeling was performed with a commercially available stereolithograph (SLA 250). A detailed description of the methodology of stereolithography has been published previously (9,14,15). Briefly, the system uses a continuous ultraviolet 325-nm helium-cadmium-multimode laser with a beam diameter of 0.24 mm. An optical system containing several dynamic mirrors directs the laser beam to the surface of the processing chamber. This chamber is filled with a liquid polyacrylic polymer, which solidifies upon heating, by the laser. A control computer (IBM compatible, Pentium CPU, 166 MHz) steers the laser beam (x, y axis) to polymerize areas on the surface layer according to the multidimensional digital ultrasound images. Successive layers (z axis) are added by means of an auto-leveling system, which incrementally lowers the platform on which the model is built to expose a new surface layer (Fig. 2).

**Validation and comparison. IN VITRO STUDIES.** Volumes of liver specimens and balloons were compared with those obtained from the acrylic models using the water-displacement method. To analyze the accuracy with which the system is able to create models, an analysis of size and geometry was performed. This was done by comparing the maximal height, width and thickness of the liver specimens to their corresponding models.

**IN VIVO STUDIES.** Evaluation and interpretation of the reconstructed cardiac structures was performed by two blinded observers. The observers were provided with both a systolic and a diastolic model of the MV and were required to determine the diagnosis (i.e., mitral stenosis, MV prolapse) and the location of the defect according to the topographical classification of MV proposed by Carpentier et al. (16).

**Statistical analysis.** All values are expressed as mean ± SD. Correlations of measurements obtained from the hard-copy replicas and the actual phantoms and from the liver specimens were assessed by linear regression analysis. The limits of agreement were assessed as described by Bland and Altman (17).

## RESULTS

**In vitro studies using balloon phantoms and liver specimens.** Modeling of all balloon phantoms and liver specimens could be performed. Mean image resolution (421 × 421 pixels) was 35.4 pixels/cm (range 22 to 54), mean slice thickness (z axis) was 0.840 mm (range 0.563 to 0.988 mm). An excellent agreement was found for volume measurements between the phantoms and their corresponding models ($r = 0.98$, SEE [standard error of the estimate] = 3.46 $mm^3$, mean difference = $-0.25 \pm 3.33$ $mm^3$). Figure 3 depicts the regression analysis and the corresponding Bland-Altman plots for volume measurements. As shown in Figure 3, an excellent agreement was also found for the comparison of the maximal dimensions (length, width and height) of the liver specimen and the corresponding models ($r = 0.99$, SEE = 0.16 cm, mean difference = $-0.03 \pm$

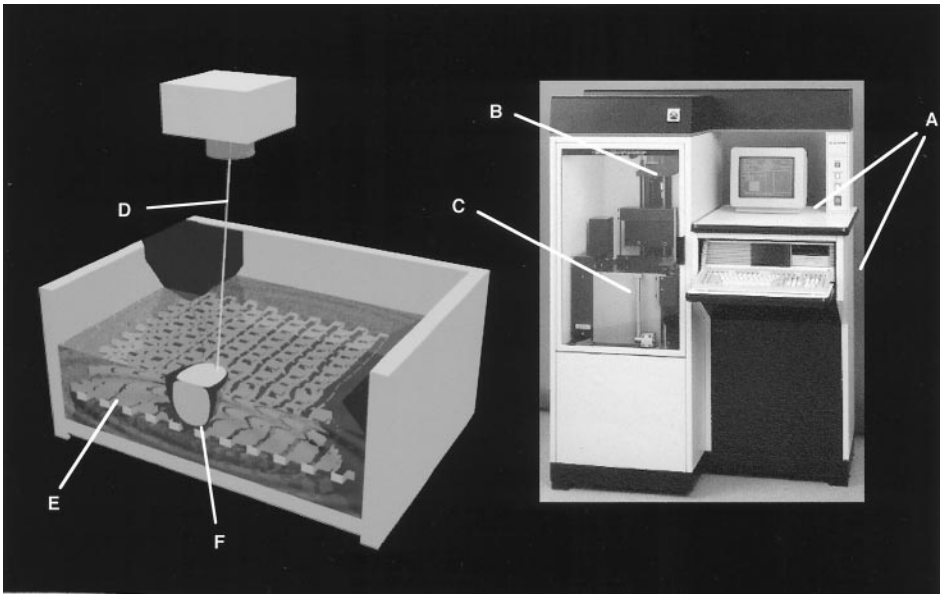


**Figure 2.** Stereolithograph: The stereolithographic equipment **(right)** consists of a computer workstation (**A**, controller), a laser with an optical system **(B)** and a processing chamber **(C)**. The processing chamber **(left)** is filled with a liquid monomer. A laser beam **(D)** selectively polymerizes ultraviolet sensitive liquid resin **(E)** on a platform suspended in a vat of the liquid. The laser is steered to corresponding positions on the surface of the liquid polymer according to the echocardiographic image (x, y axis). Successive layers (z axis) are added by lowering the platform on which the model is built to expose a new surface. Each layer fuses to the one below, allowing the creation of complex 3D structures **(F)**.

0.16 cm). Representative images of the balloon phantoms, liver specimens and their stereolithographic models are shown in Figures 4 and 5.

**In vivo evaluation of mitral valves.** Twelve of 14 (86%) studies were suitable for 3D imaging; one patient had to be excluded owing to intermittent atrial fibrillation, which did not permit RR interval thresholding, another to displacement of the probe during acquisition, which led to artifacts in the reconstructed data set. Twenty-four models of MVs (systolic frame n = 12, diastolic frames n = 12) were created. The morphology of the MV in each of these studies is listed in Table 1. The images had an average x, y resolution of 20.846 pixels/cm ± 6.68 (range 12.339 to 20.845) and an average slice thickness (z) of 1.045 mm ± 0.358 (range 0.641 to 1.62 mm).

All 24 models accurately depicted MV anatomy (Fig. 6) and pathology (Figs. 7 and 8) and allowed visual and tactile examination of each specimen and identification by the blinded observers. Models of systolic frames clearly demonstrated the presence of MV prolapse and/or flail leaflets and permitted the exact classification and location of the defect as determined by TEE (Fig. 7). A regurgitant orifice was visible in three of six (50%). Models created from diastolic frames were particularly helpful in the diagnosis of mitral stenosis (Fig. 8) and allowed the assessment of MV area and geometry. Intraoperative classification of the MV pathology as proposed by Carpentier (16) was performed in all patients who underwent surgery (n = 5). In all cases, the extent, morphology and location of the defect as described by the surgeon corresponded to the defect seen on the models (Fig. 7).

## DISCUSSION

The presented data demonstrate the feasibility, accuracy and reproducibility of using stereolithography to create high-precision, true-to-scale biomodels from 3D echocardiographic data sets. Furthermore, this study shows the potential of stereolithography to provide a detailed description of MV morphology and pathology in patients.

Stereolithography has previously been used to create models of the MV in patients with mitral stenosis (18). However, Gilon et al. (18) used a different methodology for a different purpose. They studied the effect of MV leaflet geometry on pressure and flow in such patients. In contrast to the methodology used in our study, Gilon et al. employed a transthoracic spark-gap transducer locating system and required retracing of leaflet contours to achieve wire frame reconstructions of the MV. Although this approach is suitable to study hemodynamic effects of various geometries of stenotic valves, it is less clear if such models can be used for diagnostic purposes.

**Stereolithographic modeling in comparison to 3D echocardiography.** The ability to provide tangible 3D hard-copies of cardiac structures greatly enhances visual perception. Three-dimensional imaging requires the assessment of rendering algorithms that can lead to misleading impres-

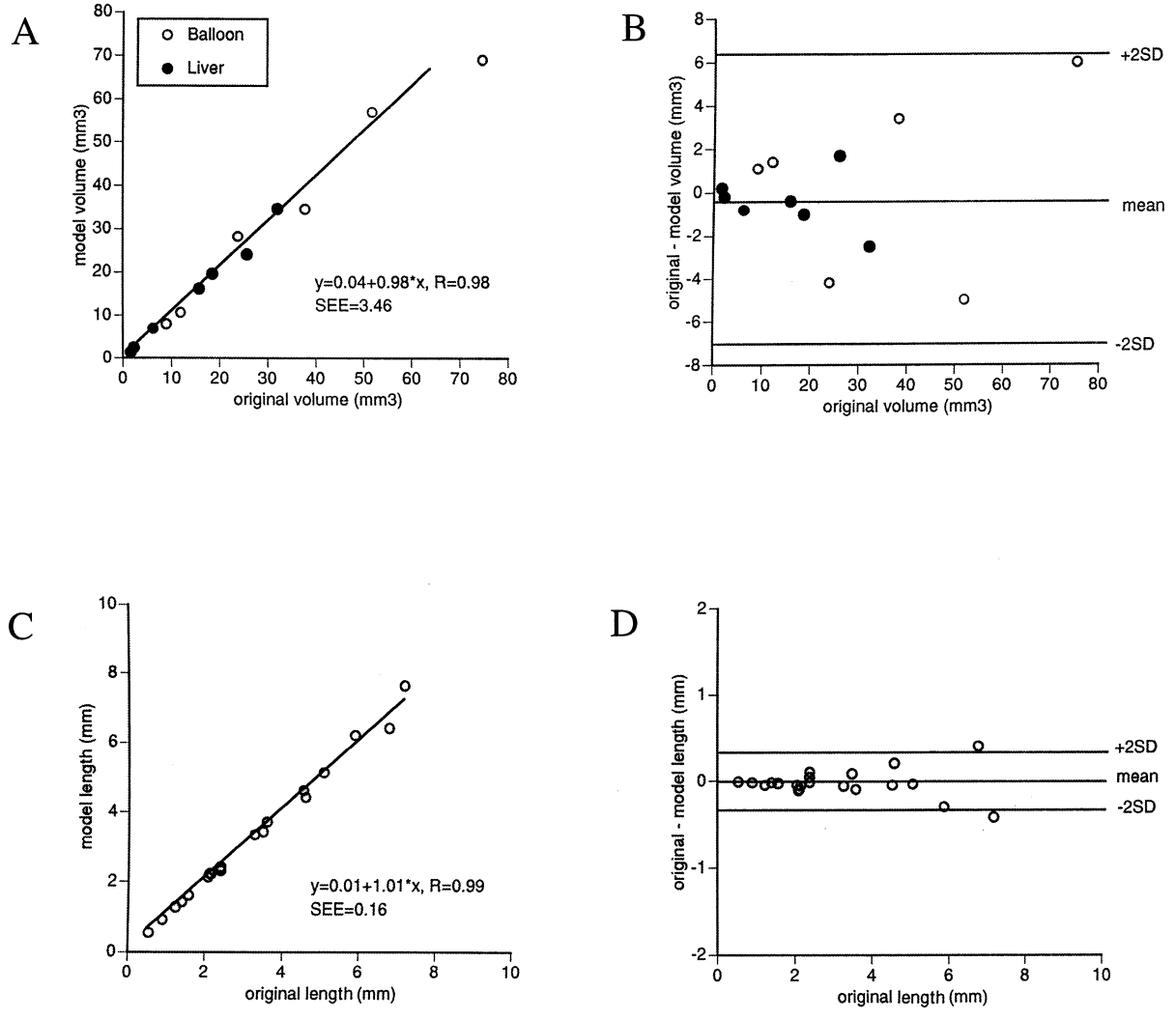


**Figure 3.** Regression analysis **(A)** and Bland Altman plot **(B)** comparing the volumes of balloon phantoms and liver specimens to their replicas. Regression analysis **(C)** and Bland-Altman plot **(D)** comparing the geometry (maximal height, width and length) of each of the liver phantoms to its corresponding model.

sions, but solid models resemble true dimensions and allow direct measurements (6). Stereolithographic models are transportable and can easily be viewed without the need of a computer and complex software. Although physicians trained in echocardiography are skillful in the interpretation of 2D scans and 3D shaded images, surgeons are not accustomed to interpret such images and may be able to obtain additional information from tangible models.

**Potential applications of stereolithographic modeling.** Although attempts to predict clinical applications of this new technology are highly speculative at best, one might anticipate that stereolithographic models could ultimately be used to facilitate preoperative planning of complex surgical procedures, including valve repair, correction of complex congenital heart disease, and complex newer procedures designed to alter the geometry of the left ventricle, such as the Batista procedure (19). Models of cardiac structures can be used as templates for surgery (i.e., for patch closure of defects or valve repair) and may ultimately offer the possibility of creating custom-built prostheses. In addition, hard-copy reconstructions could be a powerful research tool to study anatomy in different diseases and functional states (20). Finally, such models are ideal for teaching purposes and could facilitate the communication between cardiologists and patients (21).

**Technical considerations/limitations.** This method is limited by ultrasound image quality and the presence of artifacts and partial volume effects that occur during the image segmentation procedure (22). However, ultrasound image quality is greatly improved with current imaging equipment. New technologies, including contrast echocardiography, second harmonic imaging, the use of power

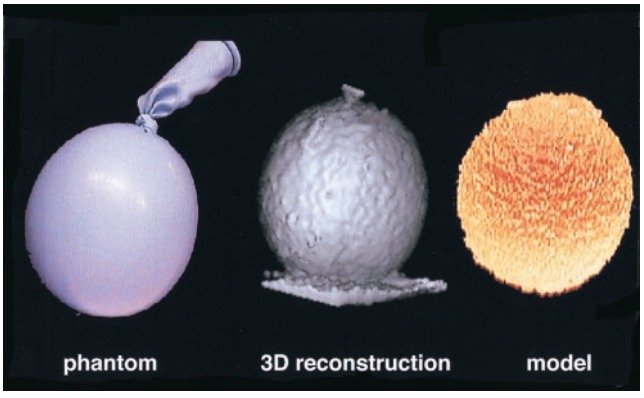


**Figure 4.** Balloon phantom **(left)**, its corresponding 3D reconstruction **(center)** and the actual photograph of the hard-copy model **(right)**.

Doppler, and pulse inversion imaging (23–25) are incorporated into many imaging devices and may further enhance the application of stereolithographic modeling.

Partial volume effects are caused by the segmentation process, which determines whether a pixel of the image corresponds to tissue or background. This task is performed by gray-scale thresholding, which classifies pixels with gray values greater than a given value (the threshold) as tissue. However, if an image voxel is occupied by both tissue and background, gray-scale averaging must be performed to determine its class membership. The resulting partial volume effect reduces the accuracy of the image (22). To compensate for these effects, gray-value interpolation is performed. However, this approach has been validated only for CT scans and might not be suitable for ultrasound images, which generally display less distinct borders. Thus, refined postprocessing algorithms might be necessary to enhance further the accuracy of stereolithographic modeling from ultrasound images.

The specimens and balloons were scanned under optimized in vitro conditions without the need to compensate for respiration and cardiac motion. Although it is more difficult to obtain adequate data sets in patients, our study demonstrated that diagnostically accurate models can also be created under clinical conditions. Nevertheless, the quality of the models greatly depends on the quality of the acquired data set. Longitudinal displacement of the probe must be avoided, a narrow electrocardiogram and respiratory trigger interval must be chosen, and overall machine settings must be optimized. As discussed above, segmentation errors

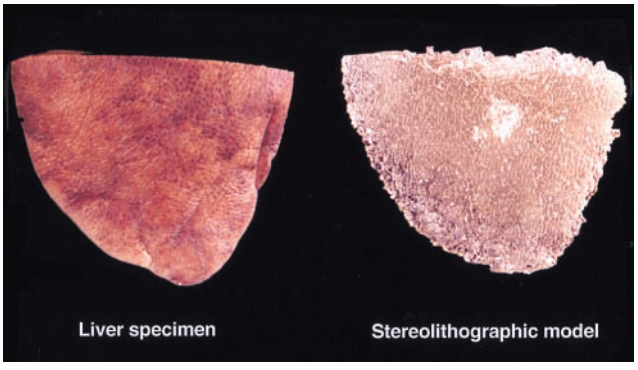


**Figure 5.** Liver specimen **(left)** and its corresponding model **(right)**.

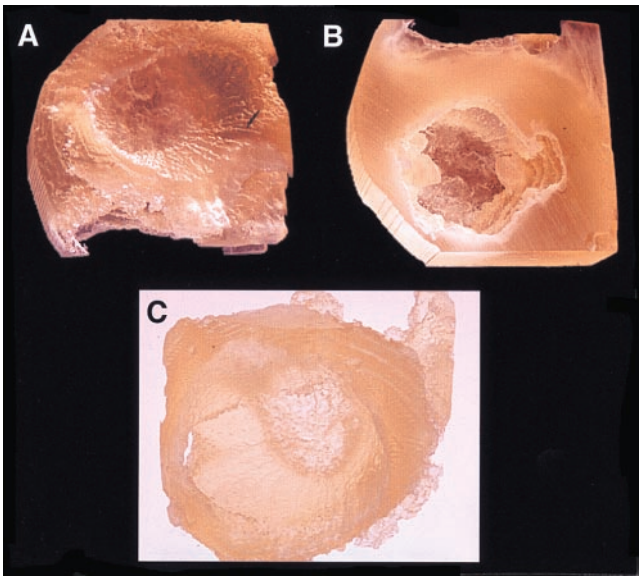


**Figure 6.** Normal MV: Stereolithographic model of a normal MV at systole as seen from the left atrium **(A)** and from the left ventricle **(B)**. Even details of the MV are clearly visible. Back light photography of the model **(C)** demonstrates the transparent appearance of the acrylic material.

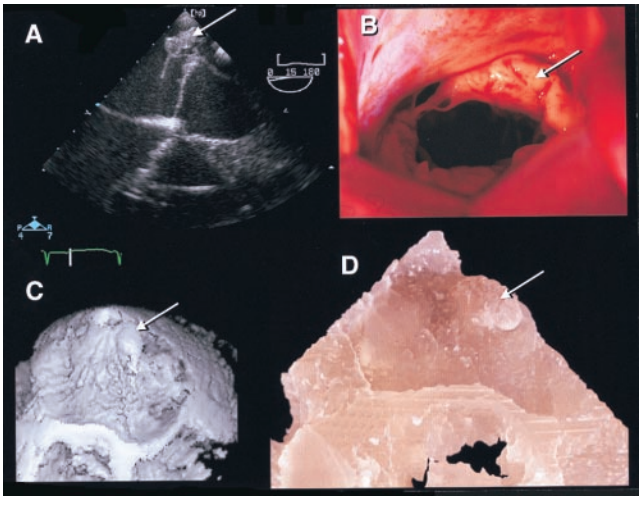


**Figure 7.** Flail posterior leaflet: Flail leaflet **(arrow)** as seen during transesophageal echocardiography **(A)** intraoperative inspection of the valve **(B)** confirmed MV prolapse, chordal rupture and a flail posterior leaflet (medial scallop). The flail segment of the posterior leaflet can be appreciated in the 3D reconstruction (at systole) **(C)** and is also visible in the stereolithographic model **(D)**.

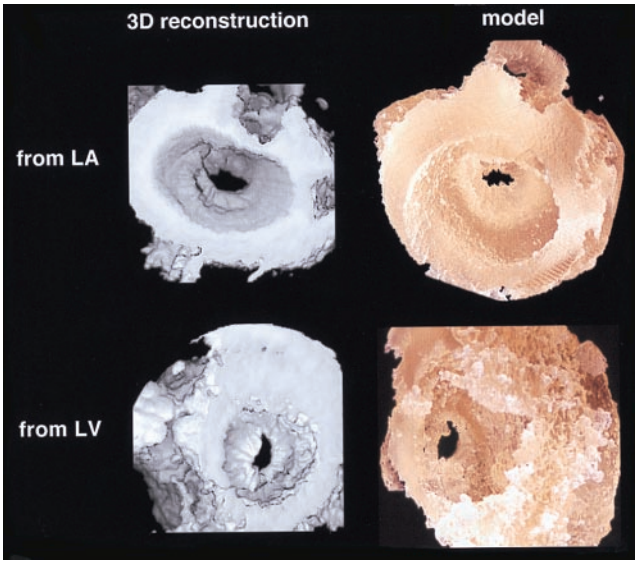


**Figure 8.** Mitral stenosis: Three-dimensional reconstructions and stereolithographic replicas of a MV with moderate to severe mitral stenosis (MVA = 1, 2 $cm^2$) during diastole as seen both from the left atrium **(top)** and from the left ventricle **(bottom)**. Note the close resemblance of the model to the 3D reconstruction. Even detailed morphologic features such as anterior MV doming or the size and geometry of the MV orifice can be appreciated.

can occur causing either dropouts (holes) or the creation of artificial structures.

The present application must be considered a prototype. However, future developments such as improvements in image quality in general, refinement of segmentation algorithms, and the advent of volumetric scanning that allows instant acquisition of a complete 3D data set could greatly enhance the practicability and accuracy of this method (26). Stereolithography is a complex off-line method, and modeling requires several hours. However, the experience in orthopedic surgery suggests that the investment in time is not a major limitation as surgery can be scheduled accordingly. Nevertheless, it will be of great importance to significantly reduce processing times. Finally, in comparison to conventional 3D computer image representation, the models do not display functional information, so that stereolithography would frequently have to be used in conjunction with conventional 3D display.

**Future developments.** To enhance the applicability of stereolithographic modeling in cardiology, future developments must be targeted to increase the resolution, enhance the speed with which models can be created, and simplify image postprocessing.

The advent of "real-time-volumetric scanning" could greatly increase the speed with which 3D echocardiographic data sets can be acquired and avoid motion artifacts caused by long acquisition times. Further improvements in image quality will also translate into more accurate models. In addition, several improvements in stereolithographic modeling are on the horizon. Whereas older materials are relatively rigid, newer acrylic materials could allow the construction of flexible models. Epoxy resins could improve the accuracy of the models below 0.1 mm (9,27), and photosensitive materials could permit the construction of multicolored models that are ideal for didactic purposes (28,29).

In conclusion, stereolithographic modeling of echocardiographic images is feasible and allows rendering of tangible polyacrylic models that are true to scale, shape and volume. Even using current technology, stereolithographic models offer accurate depiction of MV anatomy and pathology in actual patients who underwent TEE in a clinical setting. The ability to provide tangible 3D hard copies of cardiac structures should add to our spatial understanding of cardiac anatomy and physiology and could ultimately have substantial impact on diagnosis, management and preoperative planning in complex cardiovascular disorders.

**Reprint requests and correspondence:** Dr. Thomas Binder, Department of Cardiology, University of Vienna, AKH, Währingergürtel 18-20, Vienna A-1090, Austria. E-mail: thomas.binder@univie.ac.at.

## REFERENCES

1. Ghosh A, Nanda NC, Maurer G. Three-dimensional reconstruction of echocardiographic images using rotation method. Ultrasound Med Biol 1982;8:655–61.
2. Flachskampf FA, Franke A, Kuhl HP, Krebs W, Hoika J, Hanrath P. 3D-Echokardiographie: technisches Spielzeug auf der Suche nach klinischer Anwendung oder logische Weiterentwicklung des diagnostischen Instrumentariums? Z Kardiol 1997;86:336–45.
3. Binder T, Globits S, Zangeneh M, et al. Value of three-dimensional echocardiography as an adjunct to conventional transesophageal echocardiography. Cardiology 1996;87:335–42.
4. De Castro S, Yao J, Pandian NG. Three-dimensional echocardiography: clinical relevance and application. Am J Cardiol 1998;81:96G–102G.
5. Buck T, Hunold P, Wentz KU, Tkalec W, Nesser HJ, Erbel R. Tomographic three-dimensional echocardiographic determination of chamber size and systolic function in patients with left ventricular aneurysm: comparison to magnetic resonance imaging, cineventriculography, and two-dimensional echocardiography. Circulation 1997; 96:4286–97.
6. Binder T, Globits S, Zangeneh M, et al. Three-dimensional echocardiography using a transesophageal imaging probe: potentials and technical considerations. Eur Heart J 1996;17:619–28.
7. Vannan MA, Cao QL, Pandian NG, Sugeng L, Schwartz DL, Dalton MN. Volumetric multiplexed transmission holography of the heart with echocardiographic data. J Am Soc Echocardiogr 1995;8:567–75.
8. Hunziker PR, Smith S, Scherrer-Crosbie M, et al. Dynamic holographic imaging of the beating human heart. Circulation 1999;99:1–6.
9. Mankovich NJ, Cheeseman AM, Stoker NG. The display of three-dimensional anatomy with stereolithographic models. J Digit Imaging 1990;3:200–3.
10. Yau YY, Arvier JF, Barker TM. Technical note: maxillofacial biomodeling—preliminary result. Br J Radiol 1995;68:519–23.
11. Bill JS, Reuther JF, Dittmann W, et al. Stereolithography in oral and maxillofacial operation planning. Int J Oral Maxillofac Surg 1995;24(1 Pt 2):98–103.
12. Schmitt SM, Chance DA. Fabrication of titanium implant-retained restorations with nontraditional machining techniques. Int J Prosthodont 1995;8:332–6.
13. Kubler N, Michel C, Zoller J, Bill J, Muhling J, Reuther J. Repair of

human skull defects using osteoinductive bone alloimplants. J Craniomaxillofac Surg 1995;23:337–46.
14. Wolf HP, Lindner A, Millesi W, Knabl J, Watzke I. Technique and applications of stereolithographic cranial models. Fortschr Kiefer Gesichtschir 1994;39:19–22.
15. Arvier JF, Barker TM, Yau YY, Dúrso PS, Atkinson RL, McDermant GR. Maxillofacial biomodeling. Br J Oral Maxillofac Surg 1994;32: 276–83.
16. Deloche A, Jebara VA, Relland JY, et al. Valve repair with Carpentier techniques: the second decade. J Thorac Cardiovasc Surg 1990;99: 990–1002.
17. Bland JM, Altman DG. Comparing methods of measurement: why plotting difference against standard is misleading. Lancet 1995;346: 1085–7.
18. Gilon D, Cape EG, Handschumacher MD, et al. Insights from three-dimensional echocardiographic laser stereolithography: effect of leaflet funnel geometry on the coefficient of orifice contraction, pressure loss, and the Gorlin formula in mitral stenosis. Circulation 1996;9:452–9.
19. Batista RJV, Verde J, Nery P, et al. Partial left ventriculectomy to treat end-stage heart disease. Ann Thorac Surg 1997;64:634–8.
20. Otsuji Y, Handschumacher MD, Schwammenthal E. Insights from three-dimensional echocardiography into the mechanism of functional mitral regurgitation: direct in vivo demonstration of altered leaflet tethering geometry. Circulation 1997;96:1999–2008.
21. Begall K, Vorwerk U. Artificial petrous bone produced by stereolithography for microsurgical dissecting exercises. J Otorhinolaryngol Relat Spec 1998;60:241–5.
22. Goldstein A. Instrumentation of digital gray-scale US. Radiographics 1993;13:1389–95.
23. Caidahl K, Kazzam E, Lidberg J, et al. New concept in echocardiography: harmonic imaging of tissue without use of contrast agent. Lancet 1998;352:1264–70.
24. Tuchnitz A, von Bibra H, Sutherland GR, Erhardt W, Henke J, Schomig A. Doppler energy: a new acquisition technique for the transthoracic detection of myocardial perfusion defects with the use of a venous contrast agent. J Am Soc Echocardiogr 1997;10:881–90.
25. Miyatake K, Yamagishi M, Tanaka N, et al. New method for evaluating left ventricular wall motion by color-coded tissue Doppler imaging: in vitro and in vivo studies. J Am Coll Cardiol 1995;25:717–24.
26. Shiota T, Jones M, Chikada M, et al. Real-time three-dimensional echocardiography for determining right ventricular stroke volume in an animal model of chronic right ventricular volume overload. Circulation 1998;97:1897–900.
27. Berry E, Brown JM, Connell M, et al. Preliminary experience with medical applications of rapid prototyping by selective laser sintering. Med Eng Phys 1997;19:90–6.
28. Sato K, Sugawara J, Mitani H, Kawamura H. Use of selectively colored stereolithography for diagnosis of impacted supernumerary teeth for a patient with cleidocranial dysplasia. Int J Adult Orthodon Orthognath Surg 1998;13:163–7.
29. Kermer C, Rasse M, Lagogiannis G, Undt G, Wagner A, Millesi WJ. Colour stereolithography for planning complex maxillofacial tumour surgery. Craniomaxillofac Surg 1998;26:360–2.